



Adsorption of 4-Chlorophenol from Aqueous Solution onto Iraqi Bauxite and Surfactant–modified Iraqi Bauxite: Equilibrium, Kinetic, and Thermodynamic Studies

MUNA A. AL-KAZRAGI¹, DHAFIR T.A. AL-HEETIMI^{1*} and TAKIALDIN A. HIMDAN¹

¹Department of Chemistry, College of Education for Pure Science, Ibn Al-Haitham University of Baghdad, Baghdad, Iraq.

*Corresponding author E-mail: dhafir1973@gmail.com

<http://dx.doi.org/10.13005/ojc/330634>

(Received: July 10, 2017; Accepted: August 05, 2017)

ABSTRACT

Natural Bauxite (BXT) mineral clay was modified with a cationic surfactant (hexadecyltrimethyl ammonium bromide (BXT-HDTMA)) and characterized with different techniques: FTIR spectroscopy, X-ray powder diffraction (XRD) and scanning electron microscopy (SEM). The modified and natural bauxite (BXT) were used as adsorbents for the adsorption of 4-Chlorophenol (4-CP) from aqueous solutions. The adsorption study was carried out at different conditions and parameters: contact time, pH value, adsorbent dosage and ionic strength. The adsorption kinetic (described by a pseudo-first order and a pseudo-second order), equilibrium experimental data (analyzed by Langmuir, Freundlich and Temkin isotherm models) and thermodynamic parameters (change in standard free energy) (ΔG°), standard enthalpy (ΔH°), and standard entropy (ΔS°) were investigated and determined. Beside the advantages and properties of BXT-HDTMA (effective and low-cost adsorbent), the adsorption study revealed that the modification of natural bauxite (BXT) with hexadecyltrimethyl ammonium bromide has enhanced its adsorption capacity (eight to ten times greater comparison with the natural Bauxite).

Keywords: Adsorption, 4-Chlorophenol, Mineral clay, Natural Bauxite, Cationic surfactant.

INTRODUCTION

Chlorophenols are synthetic organic compounds that are used on a large scales in chemical industry including the production of pharmaceuticals, pesticides and dyes^{1,2}. They can find their way to the environment since they were detected at high concentrations in wastewater treatment plant (WWTP) and discharged effluents

close to industrial activities³. Due to the toxicity and carcinogenic properties, the long term exposure to chlorophenols at high concentration levels was found to cause liver, kidney and neurological defects, and therefore, their removal from water sources becomes environmentally warranted^{4,5}. There are different physical and chemical technologies currently used for removal phenol and its derivative compounds from their aqueous solution like oxidation⁶, adsorption⁷ and ion exchange⁸.

Adsorption is one of the most effective treatment processes to remove chlorophenols from wastewater employing different types of adsorbents such as zeolite³, sepiolite⁹, bentonite¹⁰, and carbon nano tubes¹¹. On the other hand, modified natural adsorbent were also found to be efficient in the removal of chlorophenols from its aqueous solution. For example, Al-Dujaili *et al.*,¹² used a surfactant-modified bentonite and kaolinite clays for their removal and seemed to be more effective than unmodified samples. Huang *et al.*,¹³ investigated the removal of phenol from its aqueous solution using octadecyltrimethylammonium chloride (OTMAC) modified attapulgite. The results showed that modified attapulgite can be effectively employed in the treatment of phenol-contaminated water.

Bauxite is yellowish brown solid clay mineral, very hard and high porosity¹⁴. It consists of aluminum oxide and silica with small amounts of impurities like Fe₂O₃, TiO₂, CaO, MgO, Na₂O and K₂O. The chemical characteristic of the Bauxite was formed by ternary plots of (Al₂O₃-Fe₂O₃-SiO₂)¹⁵. In general, minerals clays are known to have low content of organic carbon and hydrophilic character due to the nature of the interlayer spaces of the minerals. Thus, simple ion-exchange with surfactants results the minerals clays can convert from being organophilic to organophobic and also increases the minerals clays interlayers basal spacing¹⁶.

The aluminosilicate of clay mineral like (BXT) are negatively charged. These charges are occupied by inorganic ions like (Ca⁺² and Na⁺), which have strong hydration capability in the aqueous solutions. These mono or divalent inorganic cations can be easily replaced by positively charged organic ions (like quaternary ammonium cations) of the form [(CH₃)₃NC₁₆H₃₃]⁺ resulting in an expansion of the interparticale spacing and exposure of new sorption sites of the minerals clays¹⁷.

Therefore, in the current study, we used a cationic surfactant hexadecyl trimethyl ammonium bromide (HDTMA) for the modification of natural Bauxite surface. The isotherms, kinetics and thermodynamics of 4-Chlorophenol removal from its aqueous solution onto BXT mineral clay and a novel (BXT-HDTMA) were studied. Modified mineral clay was characterized using Fourier transform infrared (FTIR) spectroscopy, X-ray diffraction (XRD), and Scanning electron microscopic (SEM).

EXPERMANTAL

Adsorbate and Adsorbent

The adsorbate, 4-Chlorophenol was obtained from (Sigma-Aldrich ≥ 99%). The adsorbent, bauxite mineral clay was obtained from Al-Nuwaifa area at Al-Anbar governorate/Iraq. The chemical analysis was illustrated in Table 1 by using X-ray florescence spectra. The cationic surfactant Hexadecyl trimethyl ammonium bromide (HDTMA ≥ 99%) was purchased from Sigma-Aldrich. A stock solution (1000 mg/L) was prepared by dissolving 1g of 4-Chlorophenol in 1L of deionized water.

Preparation of surfactant impregnated mineral clay

The clay in powder form was washed several times with excessive amount of deionized water and then was dried at 90°C for six hours, left to cool at room temperature and then was kept in airtight container. The BXT-HDTMA was prepared by dissolving 3.5 g of HDTMA in 1L of deionized water and mixed with 50 g of bauxite and stirred for 24 hours. The suspension was then decanted, washed several times with deionized water and then dried at 90 °C for six hours. The BXT and BXT-HDTMA in this work were sieved (≤ 75µm).

Characterization of the modified adsorbent

The minerals analysis of BXT and BXT-HDTMA were characterized using X-ray diffraction (XRD) technique (Shimadzu 6000 powder diffractometer (Japan) using CuKα radiation, λ=1.5418Å at 40kV, 30 mA and 2θ range from

Table. 1: The chemical analysis of Bauxite (BXT).

Al ₂ O ₃	SiO ₂	Fe ₂ O ₃	CaO	MgO	Na ₂ O	TiO ₂	K ₂ O	L.O.I	Total %
50.64	31.03	2.75	0.04	<0.02	0.02	1.80	0.02	13.50	99.82

5-80°. The Fourier transforms infrared spectroscopy (FTIR) (Shimadzu 8400, Japan) in the wavenumber range of (4000 to 400 cm⁻¹) was used to identify the modification of BXT. Scanning electron microscope (SEM) type-T-Scan, Vega- 111(Czech) was used to determine the surface morphology of the samples

Adsorption isotherm studies

The adsorption experiments were carried out by adding 0.3 of BXT and 0.2 g of BXT-HDTMA (separately) with 10 mL of 4-Chlorophenol into conical flasks of (100 mL) at various initial concentrations of 25,50,75,100,125,150,175 and 200 mg/L. The adsorption equilibrium, adsorbent dosage, pH, ionic strength, kinetics, temperature effect at 25,35 and 45°C and thermodynamics are described below. The concentration of 4-Chlorophenol was determined by measuring the absorbance using UV-VIS spectrophotometer (T80) at 280 nm. The mass of the adsorbed sorbed amount of 4-chlorophenol (q_e, mg/g) was calculated equation (1).

$$q_e = \frac{(C_o - C_e) \times V}{W} \tag{1}$$

Where V is the volume (L) and W is the adsorbent mass dosage (g) C_o mg/L is the initial concentration and C_e mg/L the residual concentration at equilibrium). The percentage of 4-chlorophenol removal was calculated according to the equation (2).

$$\% \text{Removal (R}\%) = \frac{(C_o - C_e)}{C_o} \times 100 \tag{2}$$

RESULTS AND DISCUSSION

FTIR Spectra

The FTIR spectra for BXT and (BXT-HDTMA) are shown in figures (1a and 1b), respectively. The bands in Fig. (1a) at 3618 and 3527 cm⁻¹ can be attributed to the vibrations for the structural hydroxyl group (OH stretching). The two bands at 738 cm⁻¹ and 914 cm⁻¹ are credited to Si-O-Si and Al-O-Al bands respectively, while the band at 1033 cm⁻¹ is due to Si-O band. After modification with surfactant HDTMA Fig (1b), the bands at (3618,3527, 738 and 1033 cm⁻¹) were shifted and changed in the intensity of all bands. bands at 2920 and 2850 cm⁻¹ in modified BXT can be attributed to the symmetric and asymmetric stretching vibrations of CH₃ and CH₂ groups of the HDTMA surfactant^{18,19}.

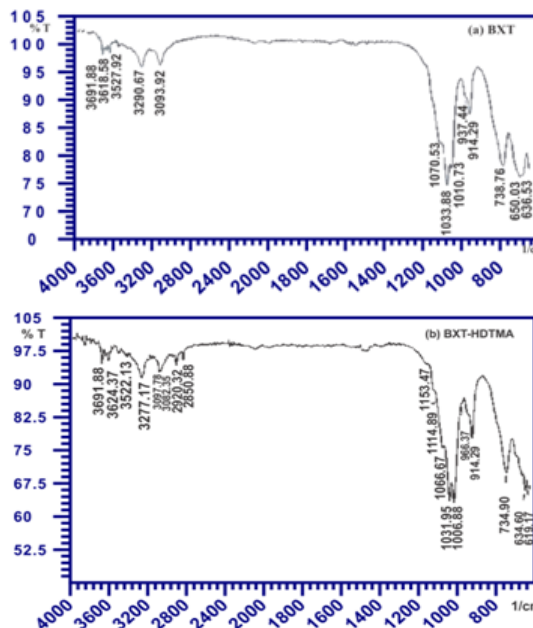


Fig.1. FTIR spectra of (a) BXT and (b) BXT-HDTMA.

SEM analysis

The scanning electron microscopic demonstrates the crystalline structure, surface texture and porosity of surface materials. The SEM micrographs of BXT and BXT-HDTMA are shown in Fig.2. The micrograph in Fig.(2a) shows that the BXT has a smooth surface with flat crystal. In Fig(2b), the mineral clay lattice is shown to be swollen and fluffy. This may be related to the increase in interparticulate spacing²⁰.

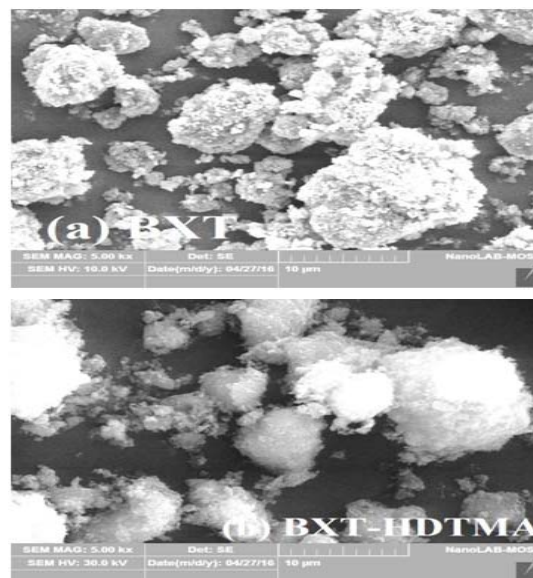


Fig.2. SEM photomicrographs for BXT(a) and BXT-HDTMA (b).

XRD analysis

The XRD analysis of BXT and BXT-HDTMA are shown in Fig. 3a and b. The differences between BXT and BXT-HDTMA modified only the intensity of the XRD peak while there is no change in BXT mineral clay indicating that the crystalline structure remained intact and has not been destroyed after the surfactant modification, as noticed from the figure, and this is in agreement with literatures^{21, 22}.

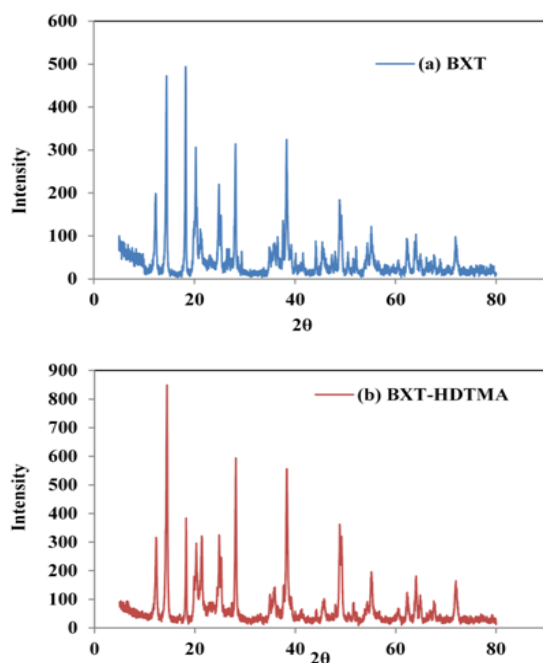


Fig.3. XRD analysis of the BXT (a) and BXT-HDTMA (b)

Adsorbent dosage effect

The effect of BXT and BXT-HDTMA dosage on the removal of 4-Chlorophenol studied at 25°C and initial concentration of 100 mg/L as shown in Fig.4. The increase in the extent of removal percentage (R%) of 4-Chlorophenol on BXT after 0.3 g of adsorbent do not effect on the removal and the adsorption is nearly constant (65%). On the other hand, the removal percentage of 4-chlorophenol increased with the increase in BXT-HDTMA dosage. This increase can be explained due to the abundance of free adsorbent sites and the high concentration gradient between the solution and the solid adsorbent²³. In addition, the increase in removal percentage (96%) can also be ascribed to the high surface area of the BXT-HDTMA due to the increase in interparticle space for BXT-HDTMA, which increases the removal capacity of adsorbent surface²⁴.

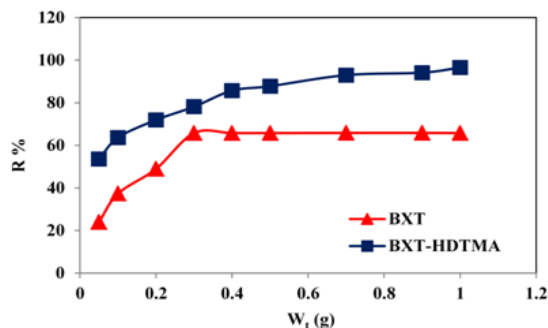


Fig.4. Effect of adsorbent dosage on the removal of 4-CP onto BXT and BXT-HDTMA at 25°C and pH 6.5.

Influence of contact Time

The influence of contact time on the adsorption of 4-CP onto BXT and BXT-HDTMA was studied at an initial concentration of 175 mg/L, 25°C, pH=6.5 and 0.3 and 0.2 g of BXT and BXT-HDTMA, respectively. Adsorption capacity of 4-CP showed an increase with time and reached a constant value at a certain time. The time required to reach equilibrium was found to be 90 and 60 min. for BXT and BXT-HDTMA, respectively, (Figure. 5).

The rapid adsorption observed at the initial stage may be related to the availability of free sites on the adsorbent surfaces. After a certain period of time, the adsorption capacity remained constant due to the less active adsorption sites being available. Notice that 4-Chlorophenol was adsorbed on BXT-HDTMA much faster BXT because the much higher affinity of the BXT-HDTMA²⁵. The surface of BXT changed from hydrophilic to hydrophobic after modification by HDTMA. Hydrophobic surface has a greater adsorption degree than hydrophilic surface for hydrophobic chemicals^{9,26,27}.

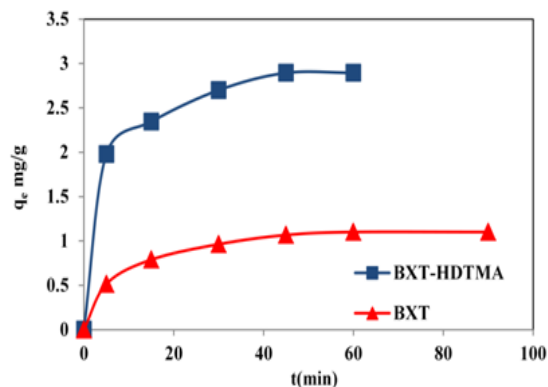


Fig. 5: Effect of contact time on adsorption of 4-CP onto BXT and BXT-HDTMA at 25°C and pH 6.5.

Influence of Ionic strength

The influence of ionic strength on the adsorption ability was studied using NaCl solution (0.05, 0.1, and 0.15 M) and 4-CP (100 mg/L) at pH = 6.5 and 25°C. The increase in ionic strength leads to increase in adsorption capacity as shown in Fig. 6. This enhancement is due to the aggregation of 4-CP by salt in solution, which decreases the volume of the molecules and increases the hydrophobicity²⁸. Moreover, the electrolyte in solution leads to decrease the repulsion between 4-CP and the surface by screening the coulombic potential between the adsorbing molecule and charged adsorbents. The higher salt concentration leads to a positive effect on the adsorption capacity of modified clay and these explain the high ability of modified Bauxite to remove the phenolic pollutant from its aqueous solution²⁹.

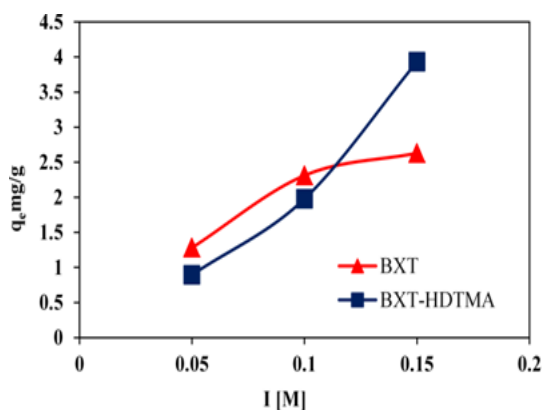


Fig.6. Effect of ionic strength on adsorption of 4-CP onto BXT and BXT-HDTMA at 25°C and pH 6.5

Influence of pH

The influence of pH on the removal of 4-CP on BXT and BXT-HDTMA was investigated at concentration of 100 mg/L, 25°C and adsorbent dosage of 0.3 and 0.2 g respectively. NaOH or HCl (0.1 M) were used to obtain the desired pH. The results are shown in Fig.7. The removal of 4-CP onto BXT and BXT-HDTMA decreased with increasing the pH towards basic medium. The total count of negatively charged surface was found to be greater at higher pH values due to the deprotonated of the surface¹⁷. This increasing in surface negative charge leads to increase the electrostatic repulsion between BXT or BXT-HDTMA and 4-CP consequently decrease the adsorption. In addition, the competitive between phenoxide ions and OH⁻ ions to active site (positive)

in surfactant can also result in a decrease in the removal percentage of 4-CP^{30,23}. At low pH, 4-CP presents the neutral form, which shows higher adsorption affinity onto BXT and BXT-HDTMA than the anionic, because the organic phase acts as an efficient partition medium for the uptake of neutral 4-CP at acidic conditions³¹.

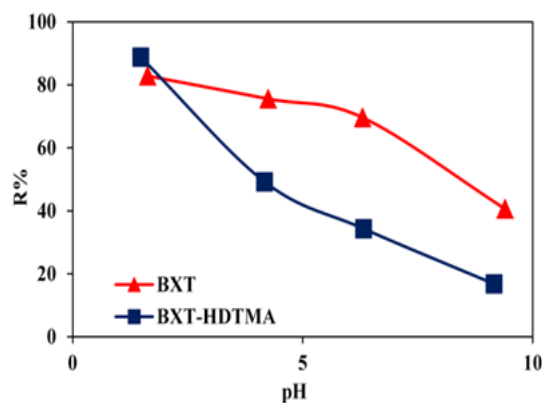


Fig.7. Effect of pH on the removal of 4-CP onto BXT and BXT-HDTMA at 25°C.

Adsorption isotherm

The adsorption of chemical compounds can be described using one of the isotherm models that can be used to describe the adsorption type and mechanism. In the current study, three isotherm models namely: Langmuir, Freundlich and Temkin models were tested in the adsorption system³².

Langmuir isotherm was the first tested model, which assumes the formation of monolayer of adsorbate on receiving surface³³. Langmuir model linear form is given in equation (3):

$$\frac{C_e}{q_e} = \frac{1}{K_L q_{max}} + \frac{C_e}{q_{max}} \quad (3)$$

Where C_e and q_e are the concentration at equilibrium (mg/L) and the quantity of 4-chlorophenol adsorbed onto BXT and BXT-HDTMA (mg/g), respectively. q_{max} is the monolayer capacity in mg/g and (K_L) is the Langmuir constant in Litre/mg. The slope $1/q_{max}$ and intercept $1/q_{max} K_L$ can be graphically calculated by plotting C_e/q_e versus C_e ³⁴.

The second tested model was Freundlich isotherm which normally used to describe the adsorption of heterogeneous systems³⁵ as expressed by the following equation(4):

$$\text{Log}q_e = \text{Log}K_F + \frac{1}{n} \text{Log}C_e \quad (4) \quad \Delta G^\circ = -RT \ln K^\circ \quad (6)$$

Where K_F (slope, mg/g) and n (intercept, unit less) are Freundlich constants and being calculated by plotting $\log q_e$ versus $\log C_e$. Finally, Temkin isotherm model was tested. This model assumes that the coverage of adsorbent surface would lead to the decrease of heat of adsorption. The Temkin isotherm can be calculated using equation (5):

$$q_e = B \ln A_T + B \ln C_e \quad (5) \quad K_d = \frac{C_o - C_e}{C_e} \times \frac{v}{w} \quad (7)$$

The plotting of q_e versus $\ln C_e$ enables the calculation of the constant A and B ³⁶.

From the values of the correlation coefficient (R^2) given in Table 2, it appears that Langmuir isotherm was found better describe the adsorption of 4-CP on BXT, While the fit of Freundlich isotherm was found to well describe the adsorption of 4-CP on BXT-HDTMA. For BXT, the maximum adsorption capacity (q_{max}) of 4-CP decreased when the temperature increased, also the adsorption energy (K_L) decreased when the all temperatures increased which indicates lower affinity between the BXT surface and 4-CP where as, the maximum adsorption capacity of 4-CP onto BXT-HDTMA decreased with the increasing of temperature and that is not agreement with experimental data³⁷.

Thermodynamic parameters

The thermodynamic parameters including Gibbs free energy (ΔG°), standard enthalpy (ΔH°), and standard entropy changes (ΔS°) were calculated using equations (6) to (8):

Where R and T are the universal gas constant and the absolute temperature (K), respectively. The equilibrium constant (K_o) was calculated as the intercept (as $\ln K_o$) of plotting $\ln K_d$ versus C_e and extrapolating C_e to 0. The distribution coefficient (K_d L/g) was calculated using the following equation (7):

The standard enthalpy change (ΔH°) and the standard entropy change (ΔS°) were calculated using the following equation (8):

$$\ln K^\circ = \Delta S^\circ / R - \Delta H^\circ / RT \quad (8)$$

The ΔH° and ΔS° were obtained by plotting $\ln K^\circ$ versus $1/T$ as the slope and intercept values as shown Fig. 8. Thermodynamic parameters for 4-CP adsorption on BXT and BXT-HDTMA are given in Table 3. The standard free energy (ΔG°) was found to be negative for two systems proves that the adsorption process are spontaneous at all temperature. The negative enthalpy change (ΔH°) suggest that the adsorption of 4-CP on BXT is an exothermic process and the negative entropy change (ΔS°) shows decrease in arbitrariness or disorder at the solid-liquid interface during the adsorption process^{38,39}, while the positive values (ΔH°) and (ΔS°) indicate that the adsorption of 4-CP on BXT-HDTMA is endothermic process and increase in disorder and randomness²⁸.

Table. 2: Langmuir, Freundlich and Temkin isotherm parameters for the adsorption of 4-CP onto BXT and BXT-HDTMA.

Isotherm	Adsorbent	298 K			308 K			318 K		
		K_L (L/mg)	q_{max} (mg/g)	R^2	K_L (L/mg)	q_{max} (mg/g)	R^2	K_L (L/mg)	q_{max} (mg/g)	R^2
Langmuir	BXT	0.013	1.721	0.995	0.011	1.696	0.991	0.009	1.628	0.969
	BXT-HDTMA	0.003	10.869	0.544	0.004	9.615	0.829	0.006	7.692	0.870
Freundlich	BXT	K_F	$1/n$	R^2	K_F	$1/n$	R^2	K_F	$1/n$	R^2
		(mg/g)			(mg/g)			(mg/g)		
	(BXT-HDTMA)	0.063	0.590	0.971	0.053	0.605	0.988	0.040	0.635	0.976
		0.056	0.819	0.986	0.067	0.804	0.994	0.100	0.739	0.994
Temkin	BXT	B	A_T	R^2	B	A_T	R^2	B	A_T	R^2
		0.389	0.124	0.994	0.371	0.109	0.983	0.342	0.098	0.975
	BXT-HDTMA	1.224	0.078	0.879	1.273	0.086	0.926	1.269	0.103	0.921

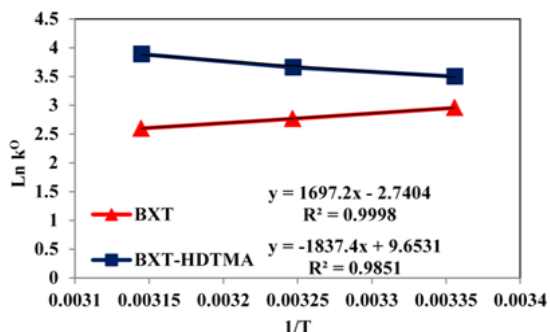


Fig.8. The relationship between $\ln K^\circ$ and $1/T$.

Adsorption kinetic models

The rate and kinetic of 4-CP adsorption onto BXT and BXT-HDTMA were tested using two kinetic models, namely: pseudo-first and pseudo-second order. The adsorption process was studied at 25, 35 and 45°C on different time intervals, pH =6.5 and an initial concentration of phenolic solution of 175 mg/L. The linear form of pseudo-first order equation is represented by equation(9)⁴⁰:

$$\ln(q_e - q_t) = \ln q_e - k_1 t \tag{9}$$

Table. 3: Thermodynamic Parameters for the adsorption of 4-CP on BXT and BXT-HDTMA.

Adsorbent	T (K)	ΔG° (kJ.mol ⁻¹)	ΔH° (kJ.mol ⁻¹)	ΔS° (kJ.° ⁻¹ .mol ⁻¹)
BXT	298	-7.32	-14.11	-22.78
	308	-7.08		
	318	-6.86		
BXT-HDTMA	298	-7.67	+15.25	+76.79
	308	-8.33		
	318	-9.21		

Where q_e , q_t and k_1 are the amounts (mg/g) of 4-CP adsorbed at equilibrium, at t time, and the rate constant of first order adsorption (min⁻¹). The value of k_1 was determined by plotting $\ln (q_e - q_t)$ versus t as shown in Figure. 9.

The pseudo-second order adsorption kinetic was extrapolated using the following equation (10):

$$\frac{t}{q} = \frac{1}{k_2 q_c^2} + \frac{t}{q_c} \tag{10}$$

Where k_2 is the rate constant of pseudo second order adsorption calculated as the slope of plotting t/q_t against time (t) as shown in Fig 10. Table 4 illustrates the pseudo-first order and pseudo-second order kinetic parameters. The values of correlation coefficient (R^2) indicate that the adsorption mechanism of 4-CP in the BXT and BXT-HDTMA systems were fitted well to the pseudo-second order model.

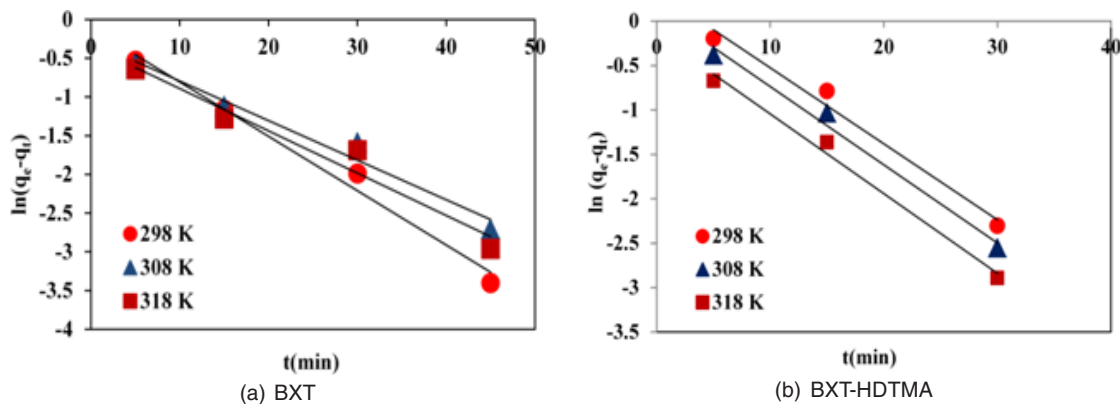


Fig.9. Pseudo-first order plot of 4-CP adsorption onto BXT(a) and BXT-HDTMA(b).

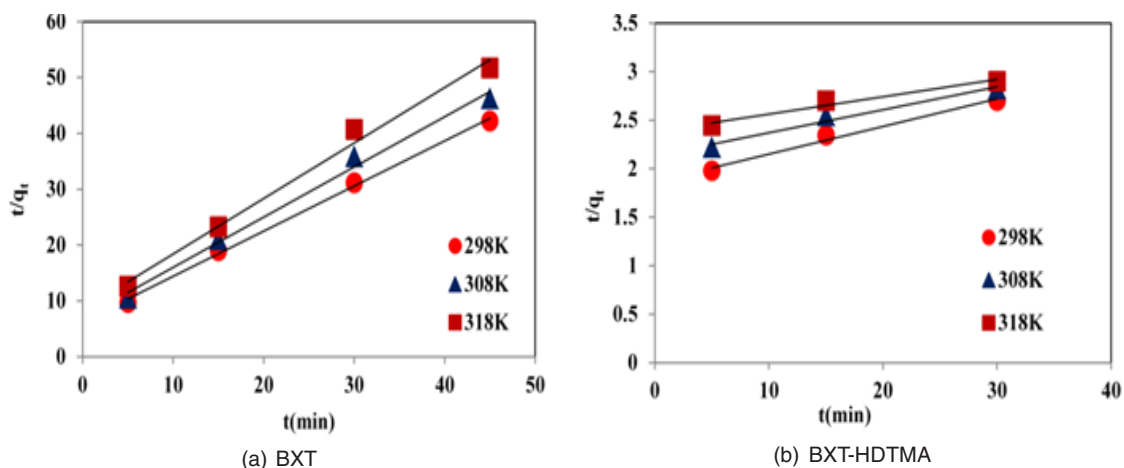


Fig.10. Pseudo-second order plot of 4-CP adsorption onto BXT(a) and BXT-HDTMA(b).

Table. 4: Kinetic parameters for the adsorption of 4-CP onto BXT and BXT-HDTMA(C_0 175 mg/L).

adsorbent	T(K)	Pseudo-first order		Pseudo-second order	
		k_1 (min^{-1})	R^2	k_2 ($\text{g} \cdot \text{mg}^{-1} \cdot \text{min}^{-1}$)	R^2
BXT	298	0.049	0.998	0.103	0.997
	308	0.051	0.971	0.114	0.991
	318	0.055	0.956	0.116	0.990
BXT-HDTMA	298	0.086	0.982	0.117	0.997
	308	0.088	0.987	0.158	0.998
	318	0.090	0.990	0.235	0.999

CONCLUSION

A new adsorbent surface (BXT-HDTMA) was synthesized and tested for the removal of 4-CP from aqueous solution. The results indicated a higher adsorption of 4-CP using the modified adsorbent (BXT-HDTMA) than unmodified natural mineral clay (BXT). The adsorption isotherm of 4-CP onto BXT was fitted with Langmuir isotherm model while the adsorption isotherm of 4-CP onto BXT-HDTMA was better described using Freundlich isotherm model.

It was obtained that the adsorption mechanism represented by pseudo second-order kinetic model for both systems. The effect of temperature was investigated and used to calculate thermodynamic parameters. The analysis of these parameters explained that the adsorption of 4-CP on BXT was spontaneous and exothermic while the adsorption of 4-CP onto BXT-HDTMA was also spontaneous but endothermic.

REFERENCES

1. Czaplicka, M., *Sci Total Environ*, **2004**, *322*(1), 21-39.
2. Igbinosa, E. O., Odjadjare, E. E., Chigor, V. N., Igbinosa, I. H., Emoghene, A. O., Ekhaise, F. O., and Idemudia, O. G., *Scientific World J.*, **2013**, *2013*,1-11.
3. Apreutesei, R. E., Catrinescu, C., Ungureanu, A., and Teodosiu, C., *Environ. Eng. Manag. J.*, **2009**,*8*(5),1053-1060.
4. Kusmierek, K., *Reaction Kinetics, Mechanisms and Catalysis*, **2016**, *119*(1), 19-34.
5. Allaboun, H. and Abu Al-Rub, F.A., *Materials*, **2016**,*9*(4):251-265.
6. Pera-Titus, M., Garcia-Molina V., Banos MA., Gimenez J. and Esplugas S., *Appl. Catal. B Environ.*, **2004**, *47*,219-256.

7. Diaz-Nava M.C., Olguin M. T., and Solache-Rios M., *J. Incl. Phenom. Macrocycl. Chem.*, **2012**, *74*, 67-75.
8. Park, Y., Ayoko, G. A., Horváth, E., Kurdi, R., Kristof, J., and Frost, R. L., *J. Colloid Interface Sci.*, **2013**, *393*, 319-334.
9. Yildiz, A., and Gür, A., *J. Serb. Chem. Soc.*, **2007**, *72*(5), 467-474.
10. Yu, J. Y., Shin, M. Y., Noh, J. H., and Seo, J. J., *Geosci. J.*, **2004**, *8*(2):191-198.
11. Ding, H., Li, X., Wang, J., Zhang, X. and Chen, C., *J. Environ. Sci.*, **2016**, *43*, 187-198.
12. Al-Dujaili, A. H., Alkaram, U. F., and Mukhlis, A. A., *J. Hazard. Mater.*, **2009**, *169*(1), 324-332.
13. Huang, J., Wang, X., Jin, Q., Liu, Y. and Wang, Y., *J. Environ. Manag.*, **2007**, *84*, 229-236.
14. Goldschmidt, V. M., *J. Am. Chem. Soc. (Resumed)*, **1937**, 655-673..
15. Power, G., Gräfe, M., and Klauber, C., *Hydrometallurgy*, **2011**, *108*(1), 33-45.
16. Ngulube, T., Gumbo, J. R., Masindi, V., and Maity, A., *J. Environ. Manag.*, **2017**, *191*, 35-57.
17. Park, Y. R., Ph.D. thesis, Queensland University of Technology, **2013**.
18. Karadag, D., Turan, M., Akgul, E., Tok, S. and Faki, A., *J. Chem. Eng. Data*, **2007**, *52*(5), 1615-1620.
19. Ma, Y., Zhu, J., He, H., Yuan, P., Shen, W., and Liu, D., *Spectrochim. Acta Mol. Spectros.*, **2010**, *76*(2), 122-129.
20. Dutta, A., and Singh, N., *Environ. Sci. Pollut. Res.*, **2015**, *22*(5), 3876-3885.
21. Hussein, M. M., Khader, K. M., and Musleh, S. M., *Inter. J. Chem. Sci.*, **2014**, *12*(3), 815-844.
22. Mao, H., Li, B., Li, X., Yue, L., Liu, Z., and Ma, W., *Ind. Eng. Chem. Res.*, **2009**, *49*(2), 583-591.
23. Zhang, L., Zhang, B., Wu, T., Sun, D., and Li, Y., *Colloid Surface A.*, **2015**, *484*, 118-129.
24. El-Dars, F. M., Hussien, M. Y. M., and Kandil, A. H. T., *Inter. J. Sci. Eng. Res.*, **2015**, *6*(3), 584-594.
25. Luo, P., Zhao, Y., Zhang, B., Liu, J., Yang, Y., and Liu, J., *Water Res.*, **2010**, *44*(5), 1489-1497.
26. Nourmoradi, H., Avazpour, M., Ghasemian, N., Heidari, M., Moradnejadi, K., Khodarahmi, F., and Moghadam, F. M., *J. Taiwan Inst. Chem. E.*, **2016**, *59*, 244-251.
27. Songül U., Atilla E., Mustafa U., Rafiö A. and Marek M., *J. Biol. Chem.*, **2015**, *43*, 235-249.
28. Wang, S., Qiao, N., Yu, J., Huang, X., Hu, M., and Ma, H., *Desalin. Water Treat.*, **2016**, *57*(9), 4174-4182.
29. Dong, L., Zhipeng, Z., and Yigang, D., *J. Disper. Sci. Technol.*, **2016**, *37*(1), 73-79.
30. Kusmieriek, K., and Swiatkowsk, A., *J. Ecol. Chem. Eng. S.*, **2015**, *22*(1), 95-105.
31. Celis, R., Koskinen, W. C., Cecchi, A. M., Bresnahan, G. A., Carrisoza, M. J., Ulibarri, M. A., and Hermosin, M. C., *J. Environ. Sci. Heal. B*, **1999**, *34*(6), 929-941.
32. Mahmoud, M. E., Nabil, G. M., El-Mallah, N. M., and Karar, S. B., *Desalin. Water Treat.*, **2016**, *57*(18), 8389-8405.
33. Atkins, P. W., physical chemistry, 8th ed. Oxford university press, **2006**.
34. Xie, J., Meng, W., Wu, D., Zhang, Z., and Kong, H., *J. Hazard. Mater.*, **2012**, *231*, 57-63.
35. Maderova, Z., Baldikova, E., Pospiskova, K., Safarik, I., and Safarikova, M., *Int. J. Environ. Sci. Te.*, **2016**, *13*(7), 1653-1664.
36. Kuleyin, A., *J. Hazard. Mater.*, **2007**, *144*(1), 307-315.
37. Mohomed, M. A., Ibrahim, A., and Shitu, A., *International Journal of Environmental Monitoring and Analysis*, **2014**, *2*, 128-133.
38. Kuo, C. Y., *Desalination*, **2009**, *249*(3), 976-982.
39. Abdelwahab, O., and Amin, N. K., *The Egyptian Journal of Aquatic Research*, **2013**, *39*(4), 215-223.
40. Dogan, M., Alkan, M., Demirbas, Ö., Özdemir, Y., and Özmetin, C., *Chem. Eng. J.*, **2006**, *124*(1), 89-101.